University of South Carolina
Scholar Commons

Faculty Publications | Chemical Engineering, Department of

1997

Ellipsometric and Raman Spectroscopic Study of Thermally Formed Films on Titanium

E. Hristova
University "Cyril and Methodius," Skopje, Macedonia

Lj. Arsov
University "Cyril and Methodius," Skopje, Macedonia

Branko N. Popov
University of South Carolina - Columbia, popov@engr.sc.edu

Ralph E. White
University of South Carolina - Columbia, white@cec.sc.edu

Follow this and additional works at: https://scholarcommons.sc.edu/eche_facpub

 Part of the Chemical Engineering Commons

Publication Info

Journal of the Electrochemical Society, 1997, pages 2318-2323.
© The Electrochemical Society, Inc. 1997. All rights reserved. Except as provided under U.S. copyright law, this work may not be reproduced, resold, distributed, or modified without the express permission of The Electrochemical Society (ECS). The archival version of this work was published in the Journal of the Electrochemical Society.
http://www.electrochem.org/
Publisher's link: http://dx.doi.org/10.1149/1.1837811
DOI: 10.1149/1.1837811

This Article is brought to you by the Chemical Engineering, Department of at Scholar Commons. It has been accepted for inclusion in Faculty Publications by an authorized administrator of Scholar Commons. For more information, please contact digres@mailbox.sc.edu.

Ellipsometric and Raman Spectroscopic Study of Thermally Formed Films on Titanium

E. Hristova and Lj. Arsov

Faculty of Technology and Metallurgy, University "Cyril and Methodius," Skopje 91000, Macedonia

B. N. Popov* and R. E. White*

Department of Chemical Engineering, University of South Carolina, Columbia, South Carolina 29208, USA

ABSTRACT

Thermal films on titanium surfaces were formed by heating titanium samples in air at atmospheric pressure. The optical constants, thickness, and structure of the formed films at various temperatures and times of heating were investigated by ellipsometry and Raman spectroscopy. The complex index of refraction and the thickness of generated films were determined by comparing the experimental loci Δ and Ψ obtained by ellipsometric measurements with theoretical computed Δ *vs.* Ψ curves. It was found that the thickness inhomogeneity and porosity of formed films increase with increasing temperature and the duration of the thermal treatment. Beyond a certain critical temperature, the appearance of some Raman bands and changes in their intensities indicated that the film transformed from amorphous to microcrystalline and crystalline structure.

Introduction

Metallic titanium and its oxides have been intensively studied during the last two decades as a result of their wide applications in various branches of industry. This metal has a high corrosion resistance due to the spontaneous formation of a thin natural film on its surface.[1] This film can be formed in atmospheric pressure at room temperature. The thickness of the films can be artificially increased by either anodically oxidizing the substrate at potentials more positive than the steady-state potentials[2] or by thermal oxidation at high temperatures.[3] Ion implantation in these oxide films causes structural amorphization and high energy lattice defects which influence the electrode capacity, the rate of electron transfer reactions, and the optical properties of the film.[4]

The optical properties and structure of anodically and thermally formed oxide films are of importance in understanding the corrosion stability and photoelectrochemical activity of titanium oxides and their applications in solar energy conversion and electrodes for electrosynthesis.[5] In recent years, the structure and optical properties of the anodic oxide films have been extensively studied by Raman spectroscopy and ellipsometry.[6,7] On the other hand, only fragmented data exist on the thermally formed oxide films utilizing Raman spectroscopy and ellipsometry.[8,9]

Most of the numerous experimental studies employ x-ray and electron diffraction techniques to investigate the crystalline structure of the thermal films. Douglass *et al.*[3] have shown the existence of titanium dioxide with rutile structure, while David *et al.*[10] have determined the structure to be both anatase and rutile modification. These discrepancies arise from the surface irregularities and the nonuniformity of the film, which is more prominent in thermally formed films at high temperatures. This is one of the primary reasons why more ellipsometric studies have been performed on anodically formed oxides than thermally formed ones.

Kozlowski *et al.*[11] showed that only rutile structure exists for thin oxide films formed at 2.5 V *vs.* a saturated calomel electrode (SCE). Since they have etched chemically the electrochemically polished surface prior to the anodic film growth, they assumed that the surface etching removes the oxide film formed during electropolishing which further strongly influences the structure of the anodic oxide film formed during electropolishing which further strongly influences the structure of the anodic oxide film. Their conclusion that the substrate surface preparation before oxidation can completely transform the crystalline structure of the anodically formed oxide film is questionable because by using chemical etching it was not possible to obtain a substrate without a naturally formed oxide film.

The objectives of this work were by using Raman spectroscopy and ellipsometry to study various structural transitions during thermal oxidation of titanium surfaces and to determine their optical properties and the crystalline structure.

Experimental

Sample preparation.—The Ti samples (99.7% pure) were machined flat in the form of disks with a diameter of 20 mm and a height of 10 mm. One base of each disk was abraded with 600 grade silicon carbide paper lubricated with distilled water. Prior to use, the disks were washed ultrasonically in alcohol and electropolished to a mirror brightness according to the procedure suggested in Ref. 12.

Heating procedure.—After electropolishing, an oxide film begins to form spontaneously on the titanium surface. Due to the high rate of contamination, it was not reasonable to study the oxidation of titanium below 100°C. On the other hand, 600°C was chosen as an upper limit because when the samples are oxidized at this temperature, the diffusion of oxygen into the bulk of the substrate becomes the rate limiting process. Due to the mass transfer limitations present at this temperature, the surface morphology becomes very inhomogeneous. This nonuniform surface creates problems with the ellipsometric measurements because the diffracted reflectance of the incident light from the Ti surface becomes more pronounced in relation with the specular one. This causes the ellipsometric measurements to begin to decrease in sensitivity and accuracy. Before thermal oxidation, ellipsometric measurements were carried out for each sample in order to determine the quality of the preliminary surface treatment. Then, the sample was placed inside a tubular oven. The temperature, measured by a thermocouple, was stabilized automatically within an accuracy of ± 1°C. The samples were heated for various times ranging from 30 s to 8 h.

After the oxidation was completed, the specimen was removed from the oven and cooled to room temperature in a desiccator. Next, ellipsometric and Raman spectroscopic tests were performed on the samples. Measurements for each oxidation time and temperature, using various samples, were repeated at least three times and the values for further computations were the average values of the single measurements. After the measurements, the oxide film was removed by mechanical means and repolished in order to reuse the sample for the next oxidation.

* Electrochemical Society Active Member.

Downloaded 22 Jul 2011 to 129.252.86.83. Redistribution subject to ECS license or copyright; see http://www.ecsdl.org/terms_use.jsp

Apparatus.—The ellipsometric analyses were executed with a Rudolph Research type 43603-200 thin film ellipsometer at a wavelength of 546.1 nm and an incident angle of 70°.

The Raman spectra were recorded by an ASCO R-800T (triple-type monochromator). The laser light for Raman excitation was 514.5 nm radiation emitted by an argon ion laser with an incident power of 10 to 15 mW. The samples were illuminated through the objective of a microscope which also served to collect the Raman light. Since the laser beam only increased the temperature of the point of illumination less than 5°C, thermal degradation of the film was not a problem.

Results and Discussion

Ellipsometry.—Ellipsometry is one of the most convenient and accurate techniques for the measurement of the thickness and refractive index of thin films on solid surfaces. In ellipsometric measurements, the oxide-free metal surface and the estimation of complex refractive index of the bare metal surface is of the most importance. An incorrect determination of the optical constants of the bare metal surface is one source of error in ellipsometric measurements. In this work, we have taken the refractive index for the oxide-free Ti surface from our previous ellipsometric measurements of electropolished and cathodically polarized Ti surfaces at −0.6 V *vs.* SCE in 0.5 *M* H_2SO_4.[6] At this potential the electrochemical reduction of natural oxide film occurred uniformly across the electrode surface. The computed values of the complex refractive index of free metal surface were $\hat{n}_s = 2.94\ (1 - 1.217i)$. These values are very close to the literature data for Ti prepared by evaporation in a vacuum and measured in high vacuum.[13] By reducing the oxide cathodically, one cannot be certain that the natural oxide film is completely reduced. According to literature, the cathodic reduction is incapable of producing an oxide-free Ti surface because of the formation of a surface hydride layer.[2]

The preliminary studies carried out to determine the influence of gas pressure on titanium oxidation reaction rate in the temperature range between 100 and 600°C showed that pressure has very little effect on the oxide film growth, indicating that the reaction between oxygen and Ti is not occurring on the base metal. Instead, the rate-determining step is probably the diffusion of oxygen atoms through a thin oxide film. Below 400°C, the titanium oxidation reaction rate (logarithmic growth rate) shows slightly noticeable variation with oxygen pressure in the range of 1 to 10 mm Hg. At 500°C and up to 600°C, the titanium oxidation reaction follows the parabolic growth rate and is independent of pressure in the range of 1 to 760 mm Hg. These results are in agreement with those obtained by Kofstadt *et al.*[14,15] and Hurlen.[16]

Figure 1 shows the variations of ellipsometric parameters Δ and Ψ during the thermal oxidation of Ti carried out at lowest investigated temperature of 100°C. By fitting the experimentally obtained points of the relative phase change Δ and the relative amplitude attenuation Ψ presented in Fig. 1 with the theoretically calculated Δ *vs.* Ψ curves, it was possible to determine accurately the thickness d and complex refractive index $[\hat{n}_2 = n_2(1 - ik_2)]$, where n_2 and k_2 are the relative index (real part) and the absorption index (imaginary part) of the thermally formed films, respectively. The theoretical Δ *vs.* Ψ curves were computed utilizing Fresnel's equations[17]

$$tg\Psi \cdot \exp(i \cdot \Delta) = \frac{r_{1,2,p} + r_{2,3,p}(-2i\delta)}{1 + r_{1,2,p} \cdot r_{2,3,p} \cdot \exp(-2i\delta)} \cdot \frac{1 + r_{1,2,s} \cdot r_{2,3,s} \cdot \exp(-2i\delta)}{r_{1,2,s} + r_{2,3,s} \cdot \exp(-2i\delta)} \quad [1]$$

$$\delta = \frac{2\pi}{\lambda} \cdot d(\hat{n}_2^2 - \hat{n}_1^2 \cdot \sin^2 \varphi_1)^{1/2} \quad [2]$$

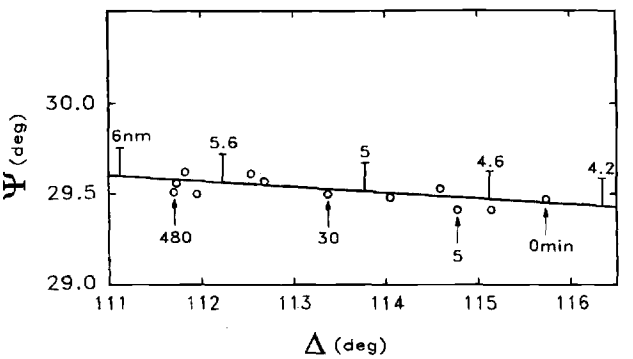

Fig. 1. Dependence of ellipsometric parameters Δ and Ψ during the thermal oxidation of Ti at 100°C. Cycles denote experimentally measured Δ and Ψ as a function of time. The solid line denotes the best theoretical fit to the experimental data computed for a growing film. A film thickness of 0 nm corresponds to the value of Δ and Ψ for a bare metal substrate.

for fixed values of the refractive index of surrounding media $\hat{n}_2$. For the surrounding media $\hat{n}_1 = 1$, while the value of the complex refractive index of metal substrate $\hat{n}_3 = 2.94\ (1 - 1.217 \cdot i)$ was taken from our previous work. In Eq. 1, $tg\Psi$ represents relative amplitude attenuation, Δ is relative phase change, r_p and r_s represent the Fresnel reflections coefficients for light polarized parallel and perpendicular to the plane of incidence, respectively, while the subscripts 1, 2, and 3 correspond to medium, film, and metal substrate, respectively. The complex refractive indexes $\hat{n}_1 = n_1\ (1 - k_1 \cdot i)$, $\hat{n}_2 = n_2\ (1 - k_2 \cdot i)$, and $\hat{n}_3 = n_3\ (1 - k_3 i)$ correspond to medium, film, and metal substrate, respectively, n_1 and k_1, n_2, and k_2 and n_3 and k_3 are relative indexes and extinction indexes of medium, film, and metal substrate. In Eq. 2, δ represents change of phase of the beam crossing the film, d is the film thickness, λ is wavelength, while φ_1 is the angle of incidence.

Figure 2 shows the variations of the ellipsometrically measured parameters Δ and Ψ during the thermal oxidation of Ti samples for the highest investigated temperature of 600°C. The refractive index, $\hat{n}_2 n$, and film thickness, d, of the formed films could be determined in the same manner as for 100°C by fitting the experimentally determined values of Δ and Ψ with theoretical computed curves. The fitting procedure was performed by a specially prepared

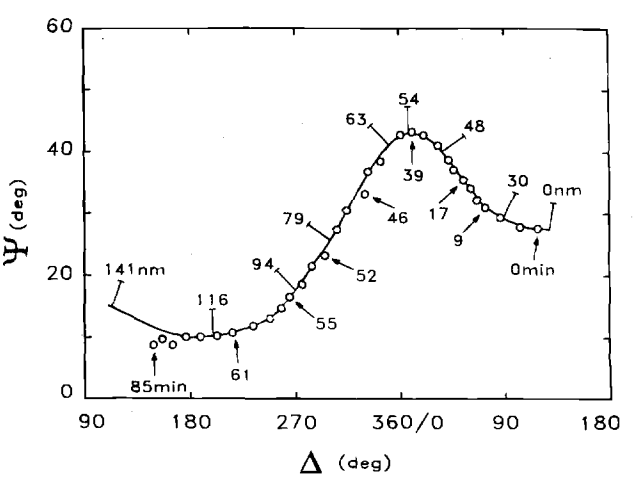

Fig. 2. Dependence of ellipsometric parameters Δ and Ψ during the thermal oxidation of Ti at 600°C. Cycles denote experimentally measured Δ and Ψ as a function of time. The solid line denotes the best theoretical fit to the experimental data computed for a growing film (thickness increments are indicated in the curve). A film thickness of 0 nm corresponds to the value of Δ and Ψ for a bare metal substrate.

Downloaded 22 Jul 2011 to 129.252.86.83. Redistribution subject to ECS license or copyright; see http://www.ecsdl.org/terms_use.jsp

computer program in which $\hat{n}_2$ was determined by given values of the film thickness in an increasing direction.[17] During the computation only one theoretical function, $T = f(\Delta_T, \Psi_T)$ was searched from the family of theoretical functions which had minimal distance to the experimental function, $E = f(\Delta_E, \Psi_E)$. When the experimentally measured Δ_T and Ψ_E were superimposed for minimal distance by computed Δ_E and Ψ_T points of theoretical curve, the fitting procedure was over. During the fitting procedure, the correct values of searched parameters were possible to obtain only if the number of theoretical points M, were many times larger than the experimentally measured values N. In this study, the number of theoretical points were at least ten times larger than those measured experimentally.

Kinetic analyses were also carried out to verify the influence of the temperature on the kinetic law of the film thickness growth. Figures 3 and 4 show the film thickness growth determined elliposmetrically during thermal oxidation at temperatures ranging from 100 to 300°C and from 400 to 600°C, respectively. The final time of the specimen thermal heating at a given temperature was determined by the noticeable variations of the position of ellipsometric parameters Δ and Ψ between two successive measurements. Next, by fitting the experimentally measured Δ *vs.* Ψ curves with theoretical ones for each temperature, the kinetic rate law of film thickness growth was determined. In order to fit the experimental kinetic data, a computer program was prepared which consists of presently known kinetic laws.[16]

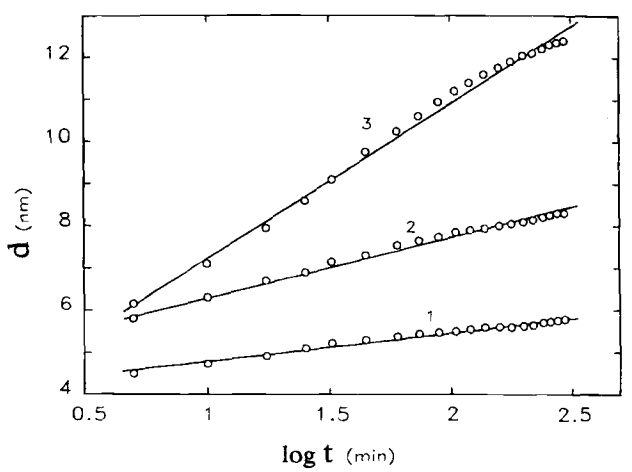

Fig. 3. Film thickness growth determined ellipsometrically during Ti heating at: (1) 100, (2) 200, and (3) 300°C.

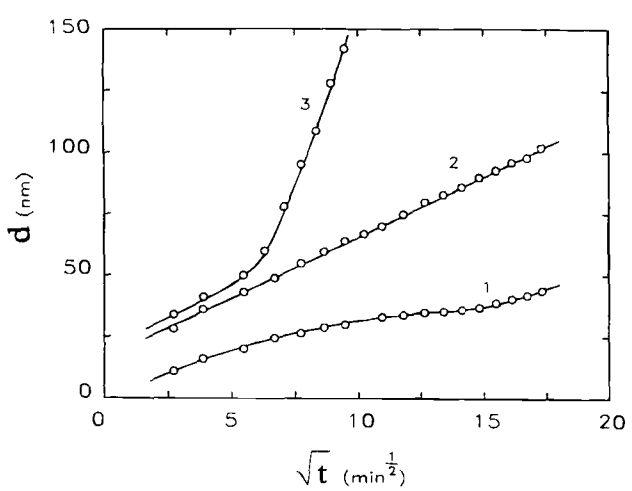

Fig. 4. Film thickness growth determined ellipsometrically during Ti heating at: (1) 400, (2) 500, and (3) 600°C.

As shown in Fig. 3, initially at temperature range of 100 to 300°C a high rate of the film thickness growth was observed. With increasing exposure time, the curves in Fig. 3 tend to level off. For a film thickness of 15 to 20 nm, the first observable interference color was yellow. At longer oxidation times and at medium temperatures, the oxidation anisotropy occurs which causes the grains to turn orange, dark brown, and finally purple. At higher temperatures there is a permanent film thickness growth which for longer oxidation time consists of grains with different color morphology and thickness.

It was found that below 375°C, the film growth can be described with the logarithmic rate law. At intermediate temperatures (375°C) the film thickness does not follow any of the known kinetic equations. At 400°C, the curve shape of the film thickness growth corresponds to the cubic rate. The experimental data obtained at 425°C were straight lines on a cubic plot, and it was difficult to determine if the oxidation was cubic or parabolic. For temperatures from 450 to 600°C, the oxidation rate can be best described as a parabolic increase in thickness. Theoretically, a parabolic rate law occurs after a logarithmic except in the case when the oxide film growth is controlled by diffusion of the ions through the film. The deviation from the parabolic rate law was accompanied by the appearance of white blisters. Curve 3 in Fig. 4, obtained at 600°C, showed (on d *vs.* $\sqrt{t}$ plot) that after the initial parabolic rate, the film growth rate changes to almost a linear rate. According to Kofstad *et al.*,[15] the activation energy for diffusion of titanium ions (in rutile), from the metal surface toward the film, is higher than the diffusion of the oxygen ions through the oxide film to the metal surface. Accordingly, the latter will predominate at lower temperatures, while diffusion of titanium ions will control the oxide growth at higher temperatures. A mechanism based on the diffusion of oxygen explains the linear oxidation. The same transformation was also observed for other metals.[19,20]

According to our microscopic studies, the oxide film formed at 100°C shows epitaxial growth. The film is compact, uniform, and it replicates the substrate grains. At temperatures between 500 and 600°C, the growth of the oxide grains is rapid; the grains are large and the film continues to show epitaxial growth. Oxidation leads to a general thickening of the oxide film and whiskers begin to form on the top of this film. At these temperatures, oxide twinning and deformation in the substrate are likely to occur.

The computed refractive indexes and the corresponding kinetic growth laws of thermally formed titanium oxide films are presented in Table I for various temperatures. According to literature, the oxide film growth up to 250°C follows logarithmic increase in thickness. Above 250°C, the oxide film growth is parabolic. However, at higher temperatures, the rate may deviate from the initial parabola, becoming linear.[21,22] There is a discrepancy in the literature about the critical temperature at which the rate low change occurs which probably results from different techniques used to study this phenomenon such as vacuum microbalance,[18] interference color method,[23] pressure change method,[24] microgravimetry,[25] and determination of absorbed oxygen on metallic surface.[21] There are a few attempts in the literature to investigate the kinetics of the oxide film growth by using ellipsometry. Boulben *et al.*[8]

Table I. Computed refractive indexes and corresponding kinetic law of thermally formed titanium oxide films at various temperatures.

Temperature (°C)	$\hat{n}_2 = n_2 (1 - ik_2)$	Kinetic law
100	$\hat{n}_2 = 2.75\ (1 - 0.001 \cdot i)$	Logarithmic
200	$\hat{n}_2 = 2.73\ (1 - 0.006 \cdot i)$	Logarithmic
300	$\hat{n}_2 = 2.71\ (1 - 0.007 \cdot i)$	Logarithmic
400	$\hat{n}_2 = 2.46\ (1 - 0.056 \cdot i)$	Transition to parabolic
500	$\hat{n}_2 = 2.40\ (1 - 0.065 \cdot i)$	Parabolic
600	$\hat{n}_2 = 2.15\ (1 - 0.111 \cdot i)$	Parabolic

Downloaded 22 Jul 2011 to 129.252.86.83. Redistribution subject to ECS license or copyright; see http://www.ecsdl.org/terms_use.jsp

carried out ellipsometric measurements in the temperature range between 300 and 420°C. They found that only parabolic rate law fits their experimental kinetic data. Contrarily, the ellipsometric kinetic data reported by Kucirek[26] fit the logarithmic law up to 480°C, while for temperatures from 600 up to 700°C the observed oxide film growth kinetic data fit the parabolic law which is in agreement with the results obtained in this study.

There are a few studies in literature regarding the variation of refractive indexes as a function of the oxide film growth. Kucirek[26] studied the variation of refractive indexes as a function of the film thickness growth for thermally formed oxide films, while Arsov *et al.*[27] studied the variation of refractive indexes of anodically formed oxide films. In this work, a detailed study was carried out to determine the effect of temperature on the values of refractive indexes. For each temperature in Table I, it was assumed that the refractive indexes n_2 and k_2 are independent of film thickness. Our assumption and the results obtained for n_2 are in good agreement with the value reported by Kucirek[26] who studied only the variation of n_2 and k_2 as a function of the film thickness growth at a fixed temperature of 600°C. According to this author the n_2 slightly decreases from 2.18 to 2.1 for a wide interval of film thickness (from 20 to 250 nm), while k_2 has constant values of about 0.05. In this study, for the same temperature, the values of n_2 and k_2 were 2.15 and 0.111, respectively. The observed difference between the k_2 value obtained in this study with the value reported by Kucirek[26] probably results from different techniques used to prepare the Ti surfaces before thermal heating. According to our previous study,[17] the electropolished Ti surface has higher values of refractive indexes of the metal substrate when compared with chemically polished surfaces. It was also found that measured refractive indexes have larger influence on k_2 than on n_2. The observed decrease of n_2 in Table I with an increase in the temperature index of air is approximately equal to one, the porous film should have a smaller refractive index, n_2, than the compact oxide film. High values observed for the absorption coefficient, k_2, at high temperatures also indicate a porous nature of these films.

For a thin oxide film, formed at a lower temperature, the values of k_2 must be very close to the nonabsorbing film. (*i.e.*, $k_2 = 0$). At higher temperatures, the oxygen ion transport number increases leading to higher internal compressive stress in the film which causes the film to lose its homogeneity. The structure of the film becomes microporous with surface defects which normally absorb more than the amorphous film before the break. Higher values of the absorption index, observed at higher temperatures also indicate an increase of the surface roughness caused by the porous structure of the film. This assumption can be verified in Fig. 2. As shown in this figure, for oxide film thickness above 130 nm, the experimental points clearly deviate from the fitted curve due to the augmentation of film porosity. Up to 130 nm, the oxide surface remained bright. With further increase of the oxide thickness, the surface became opaque. At this point the experiment was stopped because the observed complex index of refraction began to change significantly from a value of $\hat{n}_s = 2.15 (1 - 0.111 \cdot i)$ which corresponds to the theoretical computed curve.

Raman spectroscopy.—The Raman effect is a satisfactory alternative procedure to the standard x-ray and electron diffraction techniques for the detection of crystal structure. Raman spectroscopy offers the advantages of more simple sample preparation and rapidity of measurements.

The natural oxide film of an electropolished Ti surface were studied using x-ray diffraction. The measurements by short angle cameras have shown that the natural oxide film was TiO_2 with peaks for d lines which correspond to rutile structure.[28] Hugot Le-Goff[29] reported the existence of active Raman bands for very thin TiO_2 natural oxide films different than those of bulk rutile and anatase. Recently, Pankuch *et al.*[30] obtained the active Raman bands for a thin oxide film on Ti surface which indicated a high disorder of the amorphous phase consisting of TiO_2 and Ti_2O_3. Besides these studies, still the chemical composition, structure, and crystal modification of natural very thin titanium oxide films is not known.

The Raman spectra of the sample heated at a temperature of 100°C did not show any active Raman bands even after 6 h of thermal heating. Between 6 and 12 h of heating the film thickness growth was negligible (0.2 nm). Raman spectra of Ti samples heated at 500°C for 30, 180, and 360 min are shown in Fig. 5. The first visible Raman bands appear at 500°C and for an oxidation time of 30 min. At this temperature, the spectrum develops slowly and there was not a big change in the Raman bands' intensities with time, even after 6 h of heating. Only two bands appear, located at 447 and 612 cm^{-1}. These bands correspond to the E_g and A_{1g} modes of the TiO_2 rutile phase. The bands forming the rutile structure which should appear at 143 and 236 cm^{-1} are missing.

As shown in Fig. 6, the bands' intensities increased if the Ti samples were heated at a temperature of 600°C. At this temperature a complete Raman spectrum of TiO_2 with rutile structure develops within 30 min. Three strong bands, including one broad band and one shoulder, can be distinguished in the spectrum. The spectrum is stable for several days at room temperature in air. With the appearance of the first Raman bands at 500°C transformation of the oxide film from an amorphous to rutile phase begins. The Raman spectrum of a Ti sample heated to 100°C which was previously heated at 600°C showed only the bands due

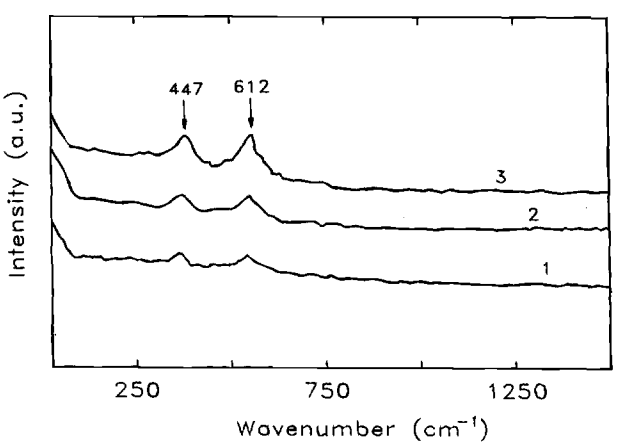

Fig. 5. Raman spectra of Ti heated for various times at 500°C. (1) 30, (2) 180, and (3) 360 min.

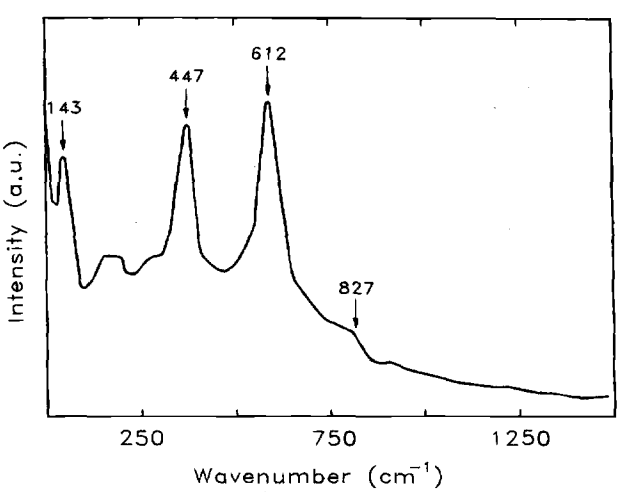

Fig. 6. Raman spectra of Ti heated at 600°C for 360 min.

Downloaded 22 Jul 2011 to 129.252.86.83. Redistribution subject to ECS license or copyright; see http://www.ecsdl.org/terms_use.jsp

to rutile structure indicating that the amorphous film transforms irreversibly to rutile structure.

The bands observed in Fig. 6 became more intense as the exposure time increases due to increased film thickness. However, the film thickness is not the only factor responsible for the intensity of Raman bands. As shown in Fig. 5, titanium oxide film with calculated thickness of 42 nm develops Raman spectrum within 30 min exposure at 500°C. On the other side, for the same oxide film thickness but at lower temperature (400°C) even after 7 h of exposure, Raman spectra were not observed indicating the importance of the substrate surface morphology and the breakdown process. When the breakdown of the film begins, the crystallization of the oxide occurs. With the progress of the breakdown the crystallite state formation also progresses causing the oxide film to become inhomogeneous. Thus, two coupled processes, surface film formation and its destruction, contribute to its inhomogeneity resulting in a number of structural defects. These defects can be observed microscopically as a variety of different interference colors which exist between the grains of the oxide. It seems that the breakdown process starts earlier than the appearance of the first Raman bands. It is still not clear if the breakdown is provoked by the oxide crystallization, or the film crystallization causes the creation of defects which are manifested as breakdown. Evidently, the conventional Raman spectroscopy is not sensitive enough to detect the earliest stages of the breakdown when the local formation of very short range structural order begins. The laser beam falls on a large surface area of the sample (about 1 mm^2), and in the Raman scattered light average values, in which amorphous structures predominate, is registered.

It is still not clear why the appearance of anatase phase is observed in anodic oxidation instead of rutile which appears in thermal oxidation of titanium. It was found by Arsov *et al.*[31] that during the anodic oxidation, the rutile structure appears after the anatase by local heating of electrode surface caused by the spark effect. The result presented in this study that the rutile is the only detected structure are not in agreement with the results obtained by David *et al.*,[10] who claim that at temperature ranges between 400 and 500°C two crystalline modifications of TiO_2, namely, both rutile and anatase, exist. The electron diffraction technique was used in their study to detect the oxide crystalline modifications. The presence of suboxides TiO_5, Ti_2O_3, and TiO were also not excluded. It is not possible for a small amount of anatase to exist in the film before detecting the rutile structure. The frequency of the most intense band, E_g mode in anatase is centered at 144 cm^{-1} which is nearly equal to that of the B_{1g} mode in rutile centered at 143 cm^{-1}. Taking into account the enormous intensity of the anatase band[7] which is approximately 30 times more intense than that one which belongs to rutile structure, it is expected that the existence of anatase in thermally formed oxide film to provoke the first appearance of the active band to be at 144 cm^{-1}, which was not observed in our studies. Also the strongest Ti_2O_3 bands which appear at 279 and 350 cm^{-1} were not detected in our study.

The results obtained in this study are in agreement with those reported by Douglas and Landuyt.[3] Using electron diffraction technique these authors have shown that on Ti samples oxidized at various times in air under atmospheric pressure and temperatures ranging between 450 and 700°C an oxide is formed with a rutile modification.

The Raman spectroscopy measurements performed so far have shown three well-known structural modifications of TiO_2: rutile, anatase, and brookite,[7,29,30] which are tetragonal, orthorhombic, and tetragonal, respectively. For rutile $\rho = 4.22$ g/cm^3, $n_2 = 2.622$; for anatase $\rho = 3.9$ g/cm^3, $n_2 = 2.544$, and for brookite $\rho = 4.23$ g/cm^3, $n_2 = 2.745$. These values are in agreement with the Pauling theory,[32] with our previous measurements carried out on anatase,[6] and with the results obtained for rutile in this study. The above data indicate that the real part of the refractive indexes decrease with decreasing density. Accordingly, the observed decrease of n_2 in Table I is caused by the decrease of the film density which results from augmentation of the porosity at higher temperatures. On the other hand, the presence of oxygen vacancies was indicated by a noticeable absorption in the visible range.[33] In both, rutile and anatase, there are two elongated titanium-oxygen bonds which occur at 0.1946 and 0.1984 nm for rutile and at 0.1937 and 0.1966 nm for anatase in each octahedron. The lengthening of these bonds is greater in the case of rutile, which causes a relative weakening of the bonds and, consequently, a lowering of the energy requirements for the excitation. This phenomenon can be correlated with the optical properties of these materials by measuring their complex refractive indexes. The vacancies are less numerous in anatase structure than in rutile, causing the value of k_2 for rutile to be bigger than the k_2 for anatase. For a thicker film with a rutile structure, the oxygen vacancies are associated with the presence of Ti ions which cause a larger porosity than in anatase and consequently larger values for k_2 than in anatase.

Conclusions

Thermal films on titanium surfaces were formed by heating titanium substrates in air at atmospheric pressure. The optical constants, thickness, and structure of the formed films at various temperatures and time of heating were investigated using ellipsometry and Raman spectroscopy.

The natural oxide film which spontaneously forms on electropolished Ti surfaces has an amorphous structure. At temperatures below 375°C, the film thickness growth can be described with the logarithmic rate law. At intermediate temperatures (375°C) the film thickness growth does not follow any of the kinetic equations. The best agreement with the experimental data was obtained with fourth degree reaction rate. At 400°C, the curve shape of the film thickness growth corresponds to the cubic rate. At 425°C, the reaction rate can be attributed as transition between cubic and parabolic rate law. For temperatures from 450 to 600°C, the oxidation rate can be best described as a parabolic increase in thickness. Up to 500°C the structure of the film is amorphous TiO_2 while above this temperature the amorphous film transforms only to rutile structure.

Manuscript submitted Aug. 8, 1996; revised manuscript received April 9, 1997.

The University of South Carolina assisted in meeting the publication costs of this article.

REFERENCES

1. Lj. Arsov, *J. Eng. Phys.*, **XX**, 5 (1979).
2. Lj. Arsov, *Electrochim. Acta*, **6**, 663 (1992).
3. D. Douglass and J. van Landuyt, *Acta Metall.*, **14**, 491 (1988).
4. L. Elfenthal, K. Leitner, and J. Schulze, *Ber. Bunsenges Phys. Chem.*, **91**, 432 (1988).
5. K. Kameyama, K. Tsukada, K. Yahikozawa, and Y. Takusu, *This Journal*, **141**, 645 (1994).
6. Lj. Arsov, *Electrochim. Acta*, **30**, 1645 (1985).
7. Lj. Arsov, C. Kormann, and W. Plieth, *J. Raman Spectrosc.*, **22**, 573 (1991).
8. J. Boulben, S. Demianiw, and J. Bardoll, *C. R. Acad. Sci., Ser. C*, 1193 (1973).
9. J. Parker and R. Siegel, *J. Mater. Res.*, **5**, 1246 (1990).
10. D. David, P. Cramery, C. Coddet, and G. Beranger, *J. Less-Common Met.*, **69**, 81 (1980).
11. M. Kozlowski, P. Tyler, W. Smyrl, and R. Atanasovski, *Surf. Sci.*, **194**, 505 (1988).
12. Lj. Arsov, M. Froelicher, M. Froment, and A. Hugot-Le Goff, *C. R. Acad. Sci., Paris*, **279**, 475 (1974).
13. P. Johnson and R. Christy, *Phys. Rev.*, **B9**, 5056 (1974).
14. P. Kofstadt and K. Hauffe, *Werkst. Korros.*, **7**, 642 (1956).
15. P. Kofstadt and K. Hauffe, *Acta Chem. Scand.*, **12**, 239 (1958).
16. T. Hurlen, *J. Inst. Metals*, **89**, 128 (1960).
17. A. Efremova and Lj. Arsov, *J. Phys., France*, **2**, 1353 (1992).
18. E. Gulbrasen and K. Andrew, *Trans. J. Amer. Electrochem. Soc.*, **96**, 364 (1949).

Downloaded 22 Jul 2011 to 129.252.86.83. Redistribution subject to ECS license or copyright; see http://www.ecsdl.org/terms_use.jsp

19. D. Davies, U. Evans, and J. Agar, *Proc. Roy. Soc.*, **225**, 443 (1954).
20. W. Vernon, E. Akeroyd, and E. Stroud, *J. Inst. Met.*, **65**, 301 (1939).
21. J. Stringer, *Acta Metall.*, **8**, 758 (1960).
22. P. Lefort, J. Desmaison, and M. Billy, *C. R. Acad. Sci., Ser. C*, 361 (1978).
23. D. McAdam and G. Geil, *J. Res. Natl. Bur. Stand.*, **28**, 593 (1942).
24. E. Gulbrasen, *Trans. Electrochem. Soc.*, **81**, 187 (1942).
25. S. Dominique, B. Devillers, and J. Bardoll, *C. R. Acad. Sci., Ser. C*, 99, (1974).
26. J. Kucirek, *C. J. Phys.*, **B23**, 1138 (1973).
27. Lj. Arsov, M. Froelicher, M. Froman, and A. Hugot Le-Goff, *Croat. Chim. Acta*, **55**, 227 (1974).
28. A. Prusi and L. Arsov, *Corros. Sci.*, **33**, 153 (1992).
29. A. Hugot Le-Goff, *Thin Solid Films*, **142**, 193 (1986).
30. M. Pankuch, R. Bell, and C. Melendres, *Electrochim. Acta*, **38**, 2777 (1993).
31. Lj. Arsov, C. Kormann, and W. Plieth, *This Journal*, **138**, 2964 (1991).
32. L. Pauling, *Z. Krist.*, **67**, 377 (1928).
33. G. Blondeau, M. Froelicher, M. Froment, and A. Hugot-Le Goff, *Thin Solid Films*, **42**, 147 (1977).

Spectroelectrochemical Study of the Role Played by Carbon Functionality in Fuel Cell Electrodes

S. C. Roy,*[a,b] A. W. Harding,[a,b] A. E. Russell,*[,b] and K. M. Thomas[a,b]

[a]*Northern Carbon Research Laboratories (NCRL) and* [b]*Department of Chemistry, University of Newcastle, Newcastle-upon-Tyne NE1 7RU, England*

ABSTRACT

X-ray absorption spectroscopy was used to identify specific types of nitrogen and sulfur-based carbon functionality present in the carbon black supports of fuel cell anodes and cathodes. The effects of these functional groups on the electrocatalytic performance of small platinum particles, dispersed on the carbon, during methanol oxidation and oxygen reduction were assessed. Electrodes functionalized with nitrogen had enhanced catalytic activities toward oxygen reduction and methanol oxidation relative to untreated electrodes. Although electrodes with sulfur functionality had higher oxygen reduction activities than untreated carbons, the activity of these electrodes toward methanol oxidation was found to be lower than electrodes manufactured from untreated carbon. It was found that carbon supports functionalized with both nitrogen and sulfur initiated the formation of Pt particles smaller in size than those observed on untreated carbon supports.

Introduction

The generation of electricity by low temperature fuel cells, such as the direct methanol fuel cell (DMFC), is increasingly perceived as an advantageous alternative to existing methods of power generation by, for example, internal combustion engines in cars. Relatively clean technology such as this will aid reduction of atmospheric pollution by generating power without the accompanying release of harmful NO_x compounds associated with fossil fuel combustion. A recent overview of underlying principles behind the DMFC can be found in Ref. 1. The electrochemical reactions taking place in the cell are oxygen reduction at the cathode and methanol oxidation at the anode. Both of these reactions occur on small particles of platinum, typically 1 to 10 nm in diameter, dispersed on a carbon black support.

The surface of the carbon black support is composed of graphene layers. Functional groups, which are predominantly oxygen, nitrogen, or sulfur based, are located at the edges of the graphene planes, or present as heteroatom functionality within the planes.[2] The design of supported catalysts, such as Pt/C, is being steadily advanced by information concerning metal-support interactions (MSIs) between surface carbon functional groups and the particulate metal. Recently, an extended x-ray absorption fine structure (EXAFS) study of Pt/C catalysts, composed of carbons impregnated with $[Pt(NH_3)_4]Cl_2$ and H_2PtCl_6,[3] has allowed distinctions to be drawn between different metal precursor-support interactions. A considerable amount of literature centered on the MSI between carbon functionality and particulate Pt, and the influence it has on particle size and dispersion can be found in Ref. 4-8. Work by Antonucci *et al.*, for example, has shown that an increase in the concentration of oxygenated carbon functional groups (*e.g.*,-COOH, -OH), as determined by x-ray photoelectron spectroscopy (XPS), decreases Pt surface area for a given loading, by increasing Pt crystallite size.[4]

Pt particle size is an important parameter which affects the reactivity of platinized fuel cell electrodes.[9] Recently, notable enhancements of short-term electrocatalytic activity toward oxygen reduction[10] have been observed on Pt/C catalysts which contain relatively small platinum crystallites. This reduction of average Pt particle size is brought about by reacting a Pt precursor solution $[Na_6Pt(SO_3)_4]$ with carbon supports containing nitrogen and sulfur functionalities. It is therefore important to be able to isolate the various types of carbon functionality present on these supports, in order to establish links between specific types of surface functionality and electrocatalytic activity.

Experiments designed to examine the nature of carbon functionality in carbonaceous materials often employ XPS.[4,11,12] Recently, XPS has been used to determine types of sulfur functionalities present in the carbon black (Vulcan XC-72) supports of fuel cell electrodes.[13] X-ray absorption near edge spectroscopy (XANES) has also been effectively used to study nitrogen and sulfur functionalities in fossil fuels.[14-17] This method has several advantages over XPS. The most notable of these is improved resolution of spectra, with less overlap of bands.

The work presented in this paper employs XANES to examine the types of carbon functionality on the carbon support and assesses electrocatalytic performance of particulate Pt dispersed on the support toward oxygen reduction and methanol oxidation. Three different types of carbon black were used: untreated, nitrogen-functionalized, and sulfur functionalized.

Experimental

Synthesis and characterization of new carbon blacks.—Introduction of sulfur to carbon black.—The Vulcan XC-72 was functionalized by addition of sulfur containing groups as described previously.[10] Briefly, a 1:2

* Electrochemical Society Active Member.

Downloaded 22 Jul 2011 to 129.252.86.83. Redistribution subject to ECS license or copyright; see http://www.ecsdl.org/terms_use.jsp